Review

Journal of Photopolymer Science and Technology
Volume 35, Number 1 (2022) 81 − 86 ©2022SPST

Chemical Mechanisms of Metal-Based Extreme Ultraviolet Resists

Albert M. Brouwer[1,2*]

[1] *Advanced Research Center for Nanolithography, P.O. Box 93019, 1090 BA Amsterdam, The Netherlands*
[2] *University of Amsterdam, van 't Hoff Institute for Molecular Sciences, P.O. Box 94157, 1090 GD Amsterdam, The Netherlands*
**a.m.brouwer@uva.nl*

Hybrid organic/inorganic materials are considered as the Extreme Ultraviolet photoresists of the future. Compared to chemically amplified polymer-based photoresists they offer higher EUV absorption cross sections, and higher etch resistance. The chemical reactions that occur in these materials upon excitation with EUV or other high energy radiation have been investigated over the past 8 years. This paper summarizes the findings for two classes of metal-based resists: metal oxo clusters with acrylate ligands, and organotin oxo cages.
Keywords: Extreme Ultraviolet, Photoresist, metal oxoclusters, tin-oxo cages, reaction mechanism

1. Introduction

Extreme Ultraviolet Lithography (EUVL) has made its entrance into the large-scale production of high-end integrated circuits. The short wavelength of light used, 13.5 nm, allows smaller features to be written in a single process step than the well-established deep UV immersion lithography (193 nm). Many technological advances have made EUVL a reality [1]. For further improvement of the productivity, advances in hardware are in progress [2], but also the "software" of photolithography, the photoresist, needs to be updated. A breakthrough in UV lithography came with the introduction of chemically amplified photoresists (CAR), in which a photochemically generated acid acts a catalyst for the ester hydrolysis that switches the solubility of the photoresist [3]. This mechanism boosts the photon efficiency and through-put of the process. For high-resolution applications, however, the catalytic step has the disadvantage that it is accompanied by diffusion and thereby leads to a blurring of the image. For today's lithographers it may be practically advantageous to adapt existing CAR materials for the use of the new wavelength of light, but for the future, other materials need to be considered. In particular, molecular hybrid organic/inorganic materials are of interest [4–7]. The metal centers in such materials can help to increase the absorption of EUV photons, and strengthen the etch resistance, allowing to apply thinner resist layers with a smaller, more favorable aspect ratio. The molecular size should allow patterning down to the nanometer scale. In contrast to the chemically amplified resists, which have a history of 40 years of research and development, the organic/inorganic materials have been investigated only recently, and there is still much to learn about how their chemistry works, and which parameters can be tuned to optimize their patterning performance. This paper will address two classes of molecular materials, namely oxo clusters of metals such as Ti, Hf, Zr, and Zn, and organotin-oxo cage compounds. First, a general picture will be sketched of the processes that take place following EUV photon absorption. Next, the current knowledge of the reaction pathways in the two classes of material will be reviewed.

When an EUV photon, with an energy of 92 eV, is absorbed by a molecule, ejection of an electron will occur [8]. Depending on the energy level (molecular or atomic orbital) from which it originates, the ejected electron may have a kinetic

Received April 30, 2022
Accepted June 24, 2022

energy up to ~85 eV. The highest energy is determined by the binding energy of the Highest Occupied Molecular Orbital. When the electron comes from a metal core level, its kinetic energy will be smaller; it is likely that the core level vacancy is filled by an Auger process releasing a second electron. In any case, the primary photoelectrons have enough kinetic energy to ionize neighboring molecules, leading to a cascade of ionization processes generating multiple electrons of lower energy, and the associated holes (one-electron oxidized molecules). In addition, electron kinetic energy may be transferred to the molecules in the resist film in the form of vibrationally and electronically excited states. While there is no doubt that all these processes take place, in general little is known about their efficiencies and relative contributions to the energy dissipation and the chemical reactivity.

The electron energy loss processes mostly take place on a short timescale, of the order of picoseconds [9]. Very few chemical reactions occur on this time scale. After this, the sample contains "holes", *radical cations* in the language of molecules, and electrons, mostly trapped in *radical anions*, and molecules in electronically excited states.

In the literature, emphasis has been placed on the electron yield [10], but the chemical reactions actually occur when bonds are broken or rearranged in the radical ions or excited molecules. The time scale for this may vary over many orders of magnitude. The radical ions can undergo reactions on the timescale of nanoseconds to milliseconds (or even longer) in competition with charge recombination. Electronically excited states (excitons) can have their specific reactions on timescales of nanoseconds to microseconds, in competition with luminescence and nonradiative decay processes. Time-resolved spectroscopies would be ideal to investigate transient species in these fast processes, but the technical requirements have precluded such experiments until now.

Our working hypothesis, based on the considerations of the previous paragraphs, is that the chemistry of molecular photoresists can -at least as a first approximation- be discussed in terms of the reactivity of the vibrationally relaxed radical ions and excited states, localized on single molecular units.

2. Metal oxoclusters

A wide variety of hybrid organic-inorganic metal oxoclusters has been reported in the recent literature [11]. To date only a few of those have been explored for EUV lithography, in particular containing Ti [12], Zr [13,14], Hf [12,15], and Zn [16,17]. Two examples are shown in Figure 1. The characteristic feature of these structures is that they have an inorganic core consisting of a number of metal atoms bridged by oxygen or OH groups, surrounded by carboxylate ligands. The carboxylate anions can be exchanged with other carboxylates, giving access to a wide variety of materials [18] with the same metal oxo core.

For lithography, the ligands of choice are methacrylates, which are well known as monomers for radical polymerization. Ample spectroscopic evidence has been presented that the C=C double bonds disappear as a result of reactions upon EUV exposure, but most of the ligands are not lost and cross-linking is the likely reaction pathway that leads to an insoluble network.

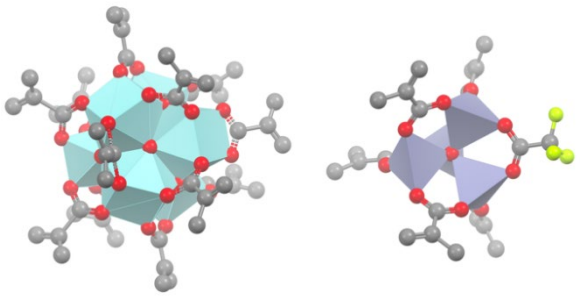

Fig. 1. Examples of oxoclusters with methacrylate ligands: $Zr_6(OH)_4O_4(OMc)_{12}$ [19] and $Zn_4O(TFA)(OMc)_5$ [17].

To form the radicals, decomposition of a fraction of the ligands is inferred (Scheme 1) as the initial step [14]. This will lead to a small loss of CO_2 which is consistent with the changes in the X-ray photoelectron spectra of the films after exposure. The loss of material via outgassing and some densification associated with the cross-linking of the ligands can be expected to lead to shrinkage of the material upon EUV-induced conversion, but this effect turns out to be small, in contrast to the case of the tin-oxo cages discussed below.

The absorption of EUV radiation by the metal oxo clusters can be enhanced by replacing hydrogen atoms in the ligands by fluorine atoms. The presence of carbon-fluorine bonds also opens a new reaction channel: a dissociative electron attachment in which a low energy electron ends up trapped in a stable fluoride anion, leaving a radical on the ligand which can initiate the cross-linking reaction. In the

case of $Zr_6O_4(OH)_4Mc_{12}$, replacement of one of the methacrylates by a trifluoromethyl acrylate led to an increased sensitivity, which may be attributable to the enhanced absorption and the additional reaction channel [20].

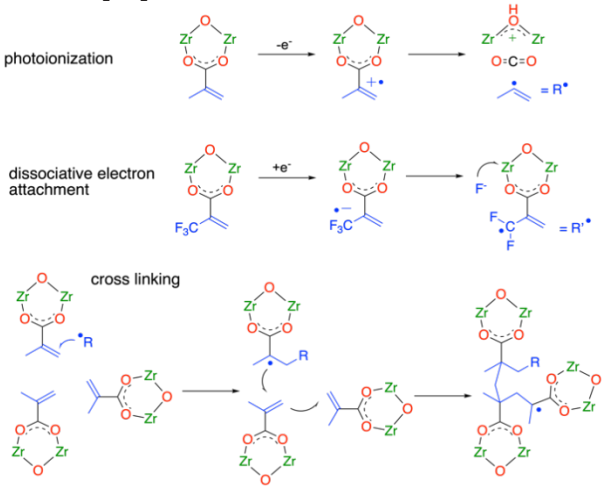

Scheme 1. Reactions occurring in (partly fluorinated) Zr MOC upon EUV excitation.

For a similar zinc-oxo cluster, however, the introduction of fluorinated methacrylates rendered the photoresist less sensitive than the parent one [21]. Here, the absorption enhancement is relatively smaller, because zinc has a higher EUV cross section than Zr, and it is counteracted by the smaller radical polymerization rate of trifluoromethyl-acrylate compared to methacrylate [22]. A practical challenge encountered with these highly fluorinated materials is in their physical properties, which affect the quality of film formation. Another noteworthy feature of this study is that the authors made an estimate of the quantum efficiency of the EUV induced conversion of the C=C double bonds to oligomers and polymers. This was found to be $\Phi \approx 10$, consistent with the formation of multiple reactive species per photon and/or a chain reaction.

Wu et al. introduced a carbazole unit in the ligand shell of the Zr_6 oxocluster [23]. This allowed to visualize the effect of EUV irradiation using fluorescence imaging. At the doses required for solubility switching, some bleaching of the organic chromophore occurred, but most of the carbazole absorption and fluorescence was retained. Interestingly, with (on average) 1 out of 12 methacrylate ligands exchanged by the carbazole ligand, the sensitivity of the material towards solubility switching was about 10× smaller than that of the parent system. Since carbazole is a strong electron donor, a likely explanation for the reduced reactivity is that potentially reactive holes are filled by electron transfer from the carbazole. Once trapped on this ligand the holes survive for a long time. This indicates that in the parent system the holes are responsible for a large part of the chemistry.

3. Organotin-oxo cages

The use of tin-oxo cages (figure 2) in EUV lithography was pioneered by the Brainard group, in the context of their MORE project [24]. In this ground-breaking work, several different organic groups connected to the Sn atoms were explored, as well as a number of different counter-ions. Negative tone EUV patterning was demonstrated, but the sensitivity appeared to be rather low. Most other researchers have restricted themselves to n-butyltin derivatives, probably because the n-butyltin precursors are commercially available. Instead of synthesizing and isolating pure tin-oxo cages, experiments have also been performed with the n-butylstannoic acid [25], and dimeric [26] and hexameric tin-oxo compounds [27]. It has been suggested that the Sn_{12} tin-oxo cages are at the basis of the EUV resist materials developed by Inpria [28,29].

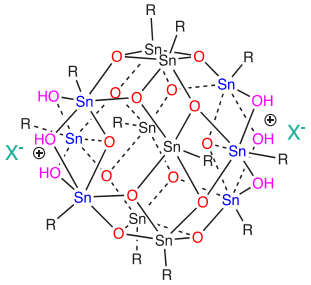

Fig. 2. General structure of Sn_{12} tin-oxo cages. R can be an aliphatic or aromatic substituent. X is a monovalent anion.

Regardless of the mode of activation, a common observation in the chemistry of organotin resists is the homolytic cleavage of the tin-carbon bond. In studies of thin resist films with methods such as infrared absorption [30], X-ray Photoelectron Spectroscopy (XPS) [25,31,32] or (near-edge) X-ray absorption spectroscopy ((NE)XAS) the loss of carbon is readily detected. It is difficult, however, to extract information on the structure of the material that remains in the exposed film. In simulation studies, it is assumed that after breaking of tin-carbon bonds, cross-linking between cages occurs, leading to the observed negative tone resist behavior [30,33,34]. The detailed chemical structures of the primary photoproducts, and the exact way they cross-link in the solid resist films, are still unknown.

In contrast to the metal oxo clusters discussed above, the sensitivity of the n-butyltin oxo cages is enhanced by post-exposure baking [35], indicating that metastable intermediates are formed after EUV irradiation that react (cross-link?) further upon heating under ambient conditions.

Some insight in the elementary steps of the photochemistry of n-butyltin oxo cages has emerged from gas phase studies of the isolated 2+ ions and their complexes with a counterion (net charge 1+) [36]. The ions were irradiated in an ion trap, with photon energies ranging from 4 eV to 35 eV, and the reaction products analyzed by means of mass spectrometry. At energies <12 eV for the bare dication and <10 eV for the complexes with one counterion, excitation can only take place to bound electronically excited states. This leads to the loss of one or two n-butyl groups. Computational quantum chemistry was used to predict the structures of the species formed. These strongly suggested that the first butyl group is lost as a radical from one of the "caps" of the rugby-ball shaped molecule. The tin-centered radical produced can easily lose a second butyl group, giving rise to a stable closed-shell product (Scheme 2).

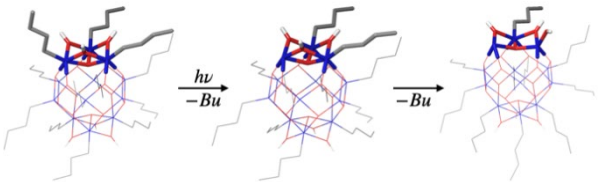

Scheme 2. Reactions occurring upon UV excitation of the tin-oxo cage dication. Two butyl groups are lost, and one bridging OH group is localized on one Sn atom [36].

It seems likely that the same products can be formed in the solid state. Direct *experimental* evidence for the structures, however, is yet to be obtained. As one of the tin atoms is formally reduced to Sn(II), oxidation reactions may take place upon heating this product in ambient conditions, which would account for the enhanced resist sensitivity following post-exposure baking that is observed experimentally [35].

At higher photon energies, the bare 2+ tin-oxo cage (>12 eV) and the 1+ complex with the counterion (>10 eV) are ionized to 3+ and 2+ radical ions, respectively. These, however, are not detected because they lose a butyl radical. When a counterion is present, it can form a bond to the formally positively charged tin atom, as illustrated in Scheme 3.

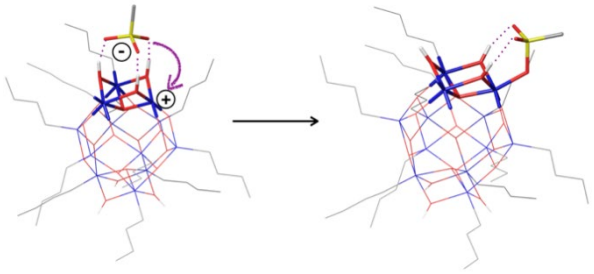

Scheme 3. Photoionization of a tin-oxo cage dication complexed with a sulfonate anion, followed by rapid loss of Bu radical, and a rearrangement of the counterion [36].

In the chemistry of the photoresist this is not likely to be a stable product, because it is still positively charged, and can be neutralized by capturing an electron, or by transferring a proton to a neighboring molecule. There are many possibilities for follow-up reactions, which remain to be investigated. Ultimately, the reaction mechanisms must account for charge neutrality, and charge recombination and (in-cage) radical recombination processes should be considered.

The gas phase studies of tin-oxo cage ions have given us some insight into the role of the counterions in the chemistry, that corroborate our earlier observations that they have a small effect on the sensitivity of the negative tone photoresist response [35]. Recently, a more dramatic effect was encountered when tin-oxo cages with very non-nucleophilic tetrakis(pentafluorophenyl)borate anions were investigated [37]. In this case at low doses a positive tone behavior was found, which implies that reaction products at low conversion are more soluble in suitably chosen developers, suggesting that cross-linking is not important in the early stages of the exposure.

When the tin-oxo cage is ionized [38], an electron is released that can initiate a cascade of events in which more electrons and holes are generated. Some of the low energy electrons can be captured by pristine tin-oxo cages. Interestingly, as shown by computation [39,40] and experiments [41], the radical anions are unstable and like the radical cations and excited states undergo cleavage of a tin-carbon bond. A difference in this case is that the bonds in the central belt of the molecule are more reactive in the reduced form, rather than the ones in the caps. Which products are formed along this pathway remains to be investigated. It is certain, however, that low energy electrons can convert the tin-oxo cage films to a large extent. This means that the reaction products of the first step can be further degraded under further loss of carbon.

4. Conclusion

Although absorption of an EUV photon delivers a large amount of energy to a molecule, the mechanisms of the solubility switching reactions in metal oxoclusters with carboxylic acid ligands and in organotin-oxo cages have been discussed on the basis of the chemistry of radicals and radical ions that result from the photoionization, electron cascade and subsequent thermalization. For the metal oxoclusters, the main reaction that switches the solubility is the cross-linking of the acrylate ligands. When the ligands contain fluorine, dissociative electron attachment pathways are opened.

For the tin-oxo cages, the primary reaction following ionization, electron capture, or electronic excitation is the cleavage of one or two tin-carbon bonds. Structures of the primary products detected via mass spectrometry of the gas phase ions have been proposed based on quantum chemical studies. A clear molecular-level mechanistic picture for the solubility switching is still lacking.

Acknowledgement

This work was performed in part in the Advanced Research Center for NanoLithography (ARCNL), a public private partnership of the University of Amsterdam (UvA), the VU University Amsterdam (VU), the Dutch Research Council (NWO) and the semiconductor equipment manufacturer ASML. Many people have made essential contributions to the research behind this paper at ARCNL, UvA, and the synchrotron facilities BESSY 2, SOLEIL, PSI and Elettra. Their names can be found as coauthors on the publications from our laboratory, a.o. references [21,31,35–38,41].

References

1. J. P. Benschop, *Proc. SPIE* **11609** (2021) 1160903.
2. H. J. Levinson, *Jap. J. Appl. Phys.* **61** (2022) SD0803.
3. H. Ito and C. G. Willson, *Polym. Eng. Sci.* **23** (1983) 1012.
4. A. Lio, *Synchrotron Rad. News* **32** (2019) 9.
5. Z. Wang, X. Yao, H. An, Y. Wang, J. Chen, S. Wang, X. Guo, T. Yu, Y. Zeng, G. Yang, and Y. Li, *J. Microelectron. Manuf.* **4** (2021) 21040101.
6. C. Luo, C. Xu, L. Lv, H. Li, X. Huang, and W. Liu, *RSC Advances* **10** (2020) 8385.
7. R. Kumar, M. Chauhan, M. G. Moinuddin, S. K. Sharma, and K. E. Gonsalves, *ACS Appl. Mater. Interfaces* **12** (2020) 19616.
8. T. Kozawa and S. Tagawa, *Jap. J. Appl. Phys.* **49** (2010) 030001.
9. C. R. Arumainayagam, H.-L. Lee, R. B. Nelson, D. R. Haines, and R. P. Gunawardane, *Surf. Sci. Rep.* **65** (2010) 1.
10. J. Torok, R. D. Re, H. Herbol, S. Das, I. Bocharova, A. Paolucci, L. E. Ocola, C. Ventrice Jr, E. Lifshin, G. Denbeaux, and R. L. Brainard, *J. Photopolym. Sci. Technol.* **26** (2013) 625.
11. U. Schubert, *Chem. Soc. Rev.* **40** (2011) 575.
12. S. Castellanos, L. Wu, M. Baljozovic, G. Portale, D. Kazazis, M. Vockenhuber, Y. Ekinci, and T. A. Jung, *Proc. SPIE* **10583** (2018) 10583A.
13. J. J. Santillan and T. Itani, *J. Photopolym. Sci. Technol.* **31** (2018) 663.
14. L. Wu, M. Baljozovic, G. Portale, D. Kazazis, M. Vockenhuber, T. Jung, Y. Ekinci, and S. Castellanos, *J. Micro/Nanolitho., MEMS, MOEMS* **18** (2019) 013504.
15. E. C. Mattson, Y. Cabrera, S. M. Rupich, Y. Wang, K. A. Oyekan, T. J. Mustard, M. D. Halls, H. A. Bechtel, M. C. Martin, and Y. J. Chabal, *Chem. Mater.* **30** (2018) 6192.
16. H. Xu, K. Sakai, K. Kasahara, V. Kosma, K. Yang, H. C. Herbol, J. Odent, P. Clancy, E. P. Giannelis, and C. K. Ober, *Chem. Mater.* **30** (2018) 4124.
17. N. Thakur, R. Bliem, I. Mochi, M. Vockenhuber, Y. Ekinci, and S. Castellanos, *J. Mater. Chem. C* **8** (2020) 14499.
18. L. Wu, J. Liu, M. Vockenhuber, Y. Ekinci, and S. Castellanos, *Eur. J. Inorg. Chem.* **2019** (2019) 4136.
19. G. Kickelbick and U. Schubert, *Chem. Ber.* **130** (1997) 473.
20. L. Wu, I. Bespalov, K. Witte, O. Lugier, J. Haitjema, M. Vockenhuber, Y. Ekinci, B. Watts, A. M. Brouwer, and S. Castellanos, *J. Mater. Chem. C* **8** (2020) 14757.
21. N. Thakur, M. Vockenhuber, Y. Ekinci, B. Watts, A. Giglia, N. Mahne, S. Nannarone, S. Castellanos, and A. M. Brouwer, *ACS Materials Au* (2022) http://dx.doi.org/10.1021/acsmaterialsau.1c00059.
22. H. Ito, D. C. Miller, and C. G. Willson, *Macromolecules* **15** (1982) 915.

23. L. Wu, M. F. Hilbers, O. Lugier, N. Thakur, M. Vockenhuber, Y. Ekinci, A. M. Brouwer, and S. Castellanos, *ACS Appl. Mater. Interfaces* **13** (2021) 51790–51798.
24. B. Cardineau, R. Del Re, M. Marnell, H. Al-Mashat, M. Vockenhuber, Y. Ekinci, C. Sarma, D. A. Freedman, and R. L. Brainard, *Microelectron. Eng.* **127** (2014) 44.
25. R. T. Frederick, S. Saha, J. T. Diulus, F. Luo, J. M. Amador, M. Li, D.-H. Park, E. L. Garfunkel, D. A. Keszler, and G. S. Herman, *Microelectron. Eng.* **205** (2019) 26.
26. N. Kenane, M. A. Grove, C. K. Perkins, T. R. Reynolds, P. H. Cheong, and D. A. Keszler, *Inorg. Chem.* **59** (2020) 3934–3941.
27. M. C. Sharps, R. T. Frederick, M. L. Javitz, G. S. Herman, D. W. Johnson, and J. E. Hutchison, *Chem. Mater.* **31** (2019) 4840.
28. S. T. Meyers, D. A. Keszler, K. Jiang, J. Anderson, and A. Grenville, US9310684B2 (2016).
29. S. T. Meyers, J. T. Anderson, B. J. Cardineau, J. B. Edson, K. Jiang, D. A. Keszler, and A. J. Telecky, US2017010612A1 (2017).
30. C. D. Needham, A. Narasimhan, U. Welling, L. S. Melvin III, P. De Schepper, J. Wouters, J. Severi, D. De Simone, and S. Meyers, *Proc. SPIE* **11323** (2020) 113230G.
31. Y. Zhang, J. Haitjema, X. Liu, F. Johansson, A. Lindblad, S. Castellanos, N. Ottosson, and A. M. Brouwer, *J. Micro/Nanolitho., MEMS, MOEMS* **16** (2017) 023510.
32. R. T. Frederick, J. T. Diulus, D. C. Hutchison, M. Nyman, and G. S. Herman, *ACS Appl. Mater. Interfaces* **11** (2019) 4514.
33. W. D. Hinsberg, and S. Meyers, *Proc. SPIE* **10146** (2017) 1014604.
34. Z. Belete, P. De Bisschop, U. Welling, and A. Erdmann, *J. Micro/Nanopattern. Mater. Metrol.* **20** (2021) 014801.
35. J. Haitjema, Y. Zhang, M. Vockenhuber, D. Kazazis, Y. Ekinci, and A. M. Brouwer, *J. Micro/Nanolitho., MEMS, MOEMS* **16** (2017) 033510.
36. J. Haitjema, L. Wu, A. Giuliani, S. Castellanos, L. Nahon, and A. M. Brouwer, *Phys.Chem.Chem.Phys* **23** (2021) 20909.
37. Q. Evrard, N. Sadegh, Y. Ekinci, M. Vockenhuber, N. Mahne, A. Giglia, S. Nannarone, T. Goya, T. Sugioka, and A. M. Brouwer, *J. Photopolym. Sci. Technol.* in press (2022).
38. Y. Zhang, J. Haitjema, S. Castellanos, O. Lugier, N. Sadegh, R. Ovsyannikov, E. Giangrisostomi, F. O. L. Johansson, E. Berggren, A. Lindblad, and A. M. Brouwer, *Appl. Phys. Lett.* **118** (2021) 171903.
39. J. H. Ma, H. Wang, D. Prendergast, A. Neureuther, and P. Naulleau, *Proc. SPIE* **11323** (2020) 113231F.
40. J. H. Ma, C. Needham, H. Wang, A. Neureuther, D. Prendergast, and P. Naulleau, *ACS Appl. Mater. Interfaces* **14** (2022) 5514–5524.
41. I. Bespalov, Y. Zhang, J. Haitjema, R. M. Tromp, S. J. van der Molen, A. M. Brouwer, J. Jobst, and S. Castellanos, *ACS Appl. Mater. Interfaces* **12** (2020) 9881.